Available online at www.sciencedirect.com
SCIENCE DIRECT®
Journal of Nuclear Materials 334 (2004) 169–179
journal of nuclear materials
www.elsevier.com/locate/jnucmat

The effect of conditioning by permanganate on the dissolution behavior of stellite particles in organic complexing acid medium

V. Subramanian [a], P. Chandramohan [a], M.P. Srinivasan [a], A.A. Sukumar [b] V.S. Raju [b], S. Velmurugan [a], S.V. Narasimhan [a,*]

[a] *Water and Steam Chemistry Laboratory, BARC Facilities, Kalpakkam, Tamilnadu 603102, India*
[b] *National Centre for Compositional Characterization of Materials, ECIL Post Hyderabad, Andhra Pradesh 500082, India*

Received 4 February 2004; accepted 25 May 2004

Abstract

Radioactive hotspots found either in the primary heat transport circuit or auxiliary circuits of nuclear reactors are mainly due to particles containing activated cobalt. The main source of these particles are stellite alloys that are rich in cobalt and are used in primary cooling circuits in valves, pumps, etc. Due to either mechanical erosion or erosion coupled with corrosion under flow conditions (known as tribocorrosion), these stellite particles are released into the system. They are then activated by neutron absorption in the reactor core before being deposited on out-of-core surfaces, causing radiation exposure problems. In this paper, the possibility of dissolving stellite particles by using an oxidation–complexation process has been explored. Permanganate based reagents were evaluated for their efficiency in conditioning the stellite particles for their dissolution with organic acids. Permanganic acid was found to be the superior conditioning agent. Two alloys of stellite, viz. stellites #3 and #6, were studied with respect to their dissolution behavior.

PACS: 28.41.Qb

1. Introduction

Stellites are Co–Cr–W alloys, which are used extensively in high-temperature applications requiring superior wear resistance and corrosion resistance. These alloys are one of the hardest materials known, having hardness numbers varying from 40 to 63 on HRC scale [1]. Many of the properties of stellites arise from the crystallographic nature of cobalt, the solid-solution strengthening effects of chromium and tungsten, and to the formation of metal carbides [2,3]. The corrosion resistance property is imparted by chromium. Stellite coated surfaces or the alloys themselves are frequently used as the material of construction for the internals of valves, pumps, etc., in water cooled nuclear reactor systems. Under high-mechanical stress, assisted by the flow of coolant, the stellite surfaces corrode and released materials comes into the neutron flux region in the core either as particles or as soluble species [4,5]. The neutron-activated particles are deposited preferentially in low-flow areas and in crevices existing in the coolant

* Corresponding author. Tel.: +91 4114 280097/280203; fax: +91 4114 280097.
E-mail address: svn@igcar.ernet.in (S.V. Narasimhan).

0022-3115/$ - see front matter © 2004 Elsevier B.V. All rights reserved.
doi:10.1016/j.jnucmat.2004.05.015

circuits giving rise to hotspots. Soluble species can get adsorbed on the coolant system structural materials. As stellite alloys are rich in cobalt, the predominant radionuclide formed by neutron activation is the long-lived ^{60}Co ($t_{1/2}$ 5.27 years) isotope. Such radioactive hot spots, due to particles containing cobalt, have been observed in many of the nuclear reactors in the world [6]. The presence of hotspots in a nuclear reactor amounts to excess costs due to an increase in the duration of shutdowns and increased complexity in the maintenance operations.

This paper gives an account of laboratory studies that were made to remove such radioactive hotspots by dissolving out the deposited stellite using a suitable chemical formulation. We have restricted ourselves to only two types of stellite that are very commonly used in the primary/moderator coolant systems of nuclear reactor systems, viz. stellites #6 and #3.

Permanganate based reagents such as alkaline permanganate, nitric acid permanganate and permanganic acid ($HMnO_4$) are generally used as a pre-treatment reagent for the decontamination of chromium containing alloys such as stainless steels, Incoloy-800 and Inconels [7]. Potassium permanganate works as an oxidizing agent both in acidic as well as in basic media. The acid permanganate oxidizes Cr(III) oxide to chromate [Cr(VI)] ions and in turn is reduced to manganese dioxide.

$$Cr_2O_3 + 2MnO_4^- + H_2O \rightarrow 2HCrO_4^- + 2MnO_2 \quad (1)$$

Similarly chromium oxide can be dissolved using alkaline permanganate as follows:

$$Cr_2O_3 + 2MnO_4^- + 2OH^- \rightarrow 2CrO_4^{2-} + 2MnO_2 + H_2O \quad (2)$$

It has been observed that acidic permanganate is more effective in conditioning the oxide film of stainless steel, whereas alkaline conditioning is suitable for Inconel-600 [8–10]. The difference was attributed to small variation in chemical composition such as more nickel, comparatively less iron and the presence of titanium in the inconel oxide.

As chromium is one of the major constituent of the stellite alloys, it is expected that permanganate based reagents would have a similar conditioning effect on these materials. Hence, an attempt has been made to investigate the effect of permanganate in acidic and alkaline media on conditioning the stellite particles and their role in the subsequent dissolution with non-oxidizing acid medium. This paper concentrates mainly on low temperature (about 60–70 °C) coolant circuits such as moderator systems and the hotspots associated with those systems. Since the amount of oxide present on the stellite particles under these conditions is negligible, this study deals with the dissolution of metallic stellite particles. Because oxidation of stellite at the high temperatures prevailing in primary/reactor coolant systems is very slow, the conclusions of this study would also be relevant to the dissolution behavior of stellite particles present there.

2. Experimental

All the chemicals used were of AR/GR grade. Solutions of nitric acid–permanganate (NP) and alkaline permanganate (AP) were prepared by mixing appropriate quantities of potassium permanganate ($KMnO_4$) and nitric acid/sodium hydroxide in double distilled water and making up to 1 l.

A stock solution of 25 mol/m^3 of permanganic acid was prepared by passing equivalent amount of potassium permanganate through cation exchange resin and then diluting it to the required concentration. Various concentrations ranging from 0.417 to 8.33 mol/m^3 were tested and were finally optimized at 2.5 mol/m^3 for the process.

2.1. Preparation and analysis of stellite powder

The stellites #6 and #3 alloys were made into chips and finely ground by using a ball-mill having tungsten carbide balls for 8 h. The composition of stellites #3 and #6 were established by X-ray florescence and atomic absorption spectrometry.

2.2. Dissolution experiments with stellite powder

2.2.1. Experimental setup

The experimental setup used in the stellite powder dissolution study consisted of a 1 l glass vessel and a heating mantle with stirrer for heating the contents of the glass vessel. Ar purging facility was provided to exclude oxygen from the atmosphere.

The stellite powder (~50 mg) was exposed to an oxidative pre-treatment step in a permanganate-based formulation for 24 h at 90 °C and samples were taken periodically and analyzed for cobalt and chromium. After the pre-oxidation step, the unused permanganate as well as the MnO_2 formed were decomposed by using citric acid that is followed by a complexation–dissolution step involving exposure to EAC (EDTA, ascorbic acid and citric acid in the weight ratio of 4:3:3) for 3 h. During the EAC step, the glass vessel was deaerated by purging with argon gas. In the dissolution experiments with stellite #3, ascorbic acid instead of citric acid was used for the neutralization of residual $HMnO_4$ at the end of the oxidation step. The concentration of chromium and cobalt were measured in the samples collected at different time intervals using atomic absorption spectrometry.

2.3. Metal dissolution rate measurements using stellite discs/rods

2.3.1. Weight loss method

Stellite #3 discs having a diameter of 6.3 mm and a thickness of 1.5 mm were polished up to 400 grit by using silicon carbide polishing papers. Similarly, stellite #6 rod of length 26 mm with a diameter of 4.5 mm was also polished up to 400 grit. Studies on the dissolution of stellite #3 were carried out using the weight-loss method by exposing it to varying concentrations of $HMnO_4$ at 90 °C followed by neutralization with ascorbic acid and treatment with EAC for 3 h. However, for stellite #6, the metal dissolution study was carried out with one concentration of $HMnO_4$ (i.e. 2.5 mol/m^3 maintained at 90 °C) and by the weight-loss method.

2.3.2. Electrochemical method

Electrochemical studies were made using an Eco Chemie Autolab PG STAT30 system. A stellite #3 disc was polished up to 800 grit, and later by using 1μm diamond paste, for working electrode. For electrochemical polarization measurements, stellite #3 was subjected to oxidizing formulation i.e. $HMnO_4$ alone. A three-electrode configuration was used with a platinum foil as the counter electrode and a saturated calomel electrode as the reference, with the potential measured through a luggin capillary.

2.4. Other instrumental techniques used

The XPS studies were carried out on stellite coupons using a VG ESCA LAB MK 200× instrument. Scanning electron microscopic (SEM) analysis of stellite particles were carried out using the SEM attachment to the same VG ESCA LAB equipment. Some of the images of stellite surfaces were taken using a PHILIPS make (model no. XL-30) SEM, with an EDX attachment. For elemental mapping, on both stellites #3 and #6 an EDAX attachment EDS–XL-30 with an ultra thin window detector and $(50 \times 50 \times 50)$ motorized u-centric stage having 10 mm working distance was used.

Particle size measurements were carried out using a MALVERN particle size measurement system.

The stellite powder, before and after the treatment with permanganic acid, as well as after the complete process ($HMnO_4$–EAC), was characterized by X-ray diffraction for phase identification. A STOE X-ray diffractometer with Cu K_α radiation was used for this purpose.

3. Results and discussions

Particle size measurements carried out on the two stellite #6 powder samples by SEM indicated that the size of the particles were in the range of 75–100 μm. Photon correlation spectroscopy (PCS) was used to determine the distribution of particle sizes in the case of stellite #3. The particle sizes had a wide distribution from 75 to 220 μm with the maximum around 140 μm. The elemental composition of these alloys as measured by atomic absorption spectrometry and X-ray fluorescence are given in Table 1 and the measured values were found to match closely with the values given in the literature. The major difference between stellites #3 and #6 is the tungsten content. In the former alloy tungsten is present to the extent of 13% where as in the latter it is only 4%. This difference in tungsten content causes marked changes in their dissolution behavior.

3.1. Powder dissolution of stellite alloys

3.1.1. Dissolution of stellite #6

Stellite #6 powder was exposed to several oxidants like nitric acid, and solutions containing a mixture of potassium permanganate and nitric acid at 90 °C. Only chromium was released to the solution during the exposure of stellite to permanganate solutions. It was observed that the rate of release of chromium during the exposure to these oxidizing reagents varied with the concentration of potassium permanganate (Table 2). The rate of chromium dissolution increased with the concentration of permanganate as it was varied in the range of 0–10 mol/m^3 with the nitric acid concentration constant at 5 mol/m^3. Similarly, experiments carried out by varying the nitric acid concentration with constant permanganate concentration indicated that chromium release is not affected by the concentration of nitric acid in solution. However, a minimum concentration of nitric acid is necessary to give the required acidity for the dissolution reaction. In both sets of experiments, subsequent to the conditioning of the stellite powder with permanganate, the solution was treated with citric acid (to convert permanganate and MnO_2 to Mn^{2+}) and then with EAC and the amount of cobalt released was measured. It was observed that the amount of cobalt released corresponded more or less with the amount of chromium released during the oxidation with the permanganate. Thus, it is very clear that it is the conditioning with permanganate that decides the extent of removal of cobalt, and unless all the chromium present in the stellite is removed, complete dissolution of cobalt cannot be achieved. With the nitric acid–permanganate solutions complete dissolution of chromium from stellite #6 could not be achieved. The reason may be that the stellite #6 alloy consists of several phases such as chromium carbides, intermetallic compounds, etc. As the chromium is released from the stellite #6, the cobalt, tungsten, etc., are left behind in the residue. In addition, some phases that contain chromium also remain undissolved during their exposure to the mixture containing nitric acid and potassium permanganate.

Table 1
Elemental composition of stellite alloys

Element	Literature [1]		Estimated	
	Stellite #6 (wt%)	Stellite #3 (wt%)	Stellite #6 (wt%)	Stellite #3 (wt%)
Co	62	48.8	60	49
Cr	28	32	33	31
Ni	<3	<3	0.24	1.8
Fe	3	<3	–	1.4
W	4	13	3.6	13
C	1	2.4	–	–
Si	1	1	–	–
Insoluble	–	–	6	–

Table 2
Percentage of cobalt and chromium dissolved from stellite #6 after pre-treatment with various NP formulations followed by ascorbic acid and EAC

Formulation	Cr (% dissolution)	Co[a] (% dissolution)
5 mol/m^3 HNO_3	–	5
5 mol/m^3 HNO_3, 5 mol/m^3 $KMnO_4$	20	34
5 mol/m^3 HNO_3, 10 mol/m^3 $KMnO_4$	36	40
2.5 mol/m^3 HNO_3, 2.5 mol/m^3 $KMnO_4$	30	40
5 mol/m^3 HNO_3, 2.5 mol/m^3 $KMnO_4$	33	38
10 mol/m^3 HNO_3, 2.5 mol/m^3 $KMnO_4$	29	44
AP (2.5 mol/m^3 $KMnO_4$, 7.5 mol/m^3 NaOH)	–	3.5
2.5 mol/m^3 $HMnO_4$	60	89

[a] After final EAC step.

Stellite #6 dissolution was also carried out in alkaline permanganate solution having 2.5 mol/m^3 $KMnO_4$ and 7.5 mol/m^3 NaOH. Dissolution experiments carried out at 90 °C for 24 h indicated that the dissolution of chromium from stellite #6 is poor in alkaline permanganate. Exposure of the stellite #6 to EAC formulation subsequent to the alkaline permanganate also did not result in dissolution of cobalt and other elements. Thus, it is very clear that stellite #6 is not at all affected by the alkaline permanganate reagent.

Based on the studies made on certain chromium alloys namely stainless steel and Inconel-600, it has been reported that the nature of the oxide film is very crucial in deciding the relative efficiency of NP and AP to remove chromium from the oxide. The presence of non-chromium metals in the oxide layer changes its dissolution behavior in a particular formulation [8]. Chromium is present in stellite mainly as eutectic carbides of type M_7C_3, $M_{23}C_6$ and as metallic chromium in the matrix. Hence chromium release from stellite is entirely different from that of the oxide formed at elevated temperature; moreover, under low-temperature conditions the oxide layer present on stellite will be extremely thin. Once the thin layer is dissolved, the permanganate in alkaline conditions is not able to oxidize chromium from its carbide phases effectively. In NP, the dissolution is much better, probably due to its acidity.

Dissolution of stellite #6 was also attempted with permanganic acid ($HMnO_4$). The difference between nitric acid–permanganate and permanganic acid is the absence of nitrate (NO_3^-) ion in the solution. Experiments carried out with 2.5 mol/m^3 $HMnO_4$ at 90 °C indicated that in this medium the maximum amount of chromium is dissolved from stellite #6. Dissolution of the residue left after the permanganic acid treatment in citric acid/EAC also confirmed that the former is able to dissolve the chromium from the stellite #6 more efficiently than the other oxidizing reagents, and almost complete dissolution of cobalt ($\geqslant$ 90%) could then be achieved in citric acid/EAC. Thus, in the absence of nitrate ion in solution, dissolution of chromium from stellite #6 tends to go to completion. Nitrate ion can act as a passivator under certain conditions. As stellite is a multiphase alloy, one or more phases of this alloy may get passivated by nitrate ion thereby hindering the dissolution process. The results of stellite #6 dissolution in terms of percentage dissolution of cobalt are given in Fig. 1. From this figure it is very clear that the dissolution efficiency of the three permanganate reagents varies in the order $HMnO_4$ > NP > AP.

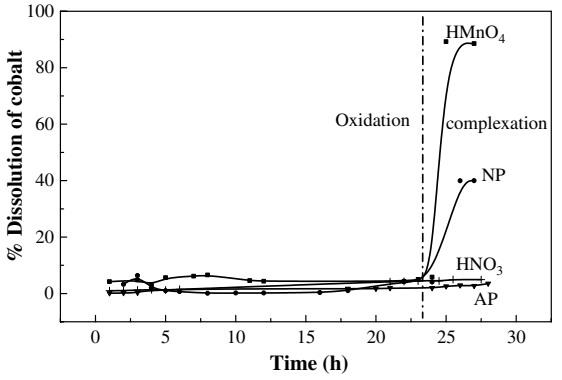

Fig. 1. Dissolution of cobalt from stellite #6 preconditioned with various oxidizing formulations followed by treatment with citric acid and EAC.

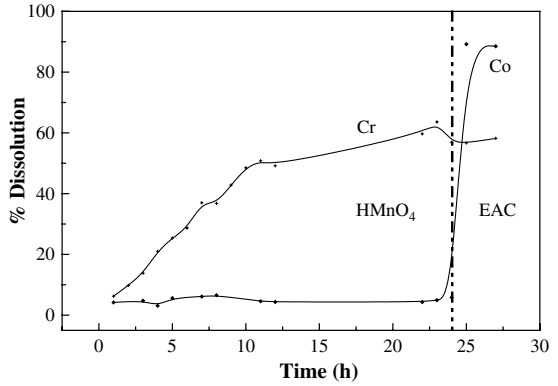

Fig. 2. Dissolution behavior of cobalt and chromium from stellite #6 in $HMnO_4$ citric acid and EAC.

Fig. 2 shows the dissolution behavior of cobalt and chromium from stellite #6 in $HMnO_4$ medium. It can be seen that most of the chromium dissolves during the oxidation step and reaches a saturation value, whereas cobalt starts coming into the solution immediately after the neutralization of permanganate with citric acid/EAC. The release of chromium from stellite #6 when exposed to permanganic acid was found to obey the inverse cubic rate law:

$$(1 - C_t/C_\infty)^{1/3} = 1 - k_{obs}t.$$

A plot of $(1 - C_t/C_\infty)^{1/3}$ vs time (Fig. 3) for chromium release in oxidizing medium shows linear behavior up to 50% dissolution with a slope that corresponds to $k_{obs} = k/\rho r_o = 0.0185$. The linear behavior implies that the rate of dissolution is proportional to the instantaneous surface area of the particle dissolving; i.e. it follows the reducing sphere model, which is used for explaining metal-oxide dissolution reactions [11]. This is quite unexpected, because the cobalt present in the stellite

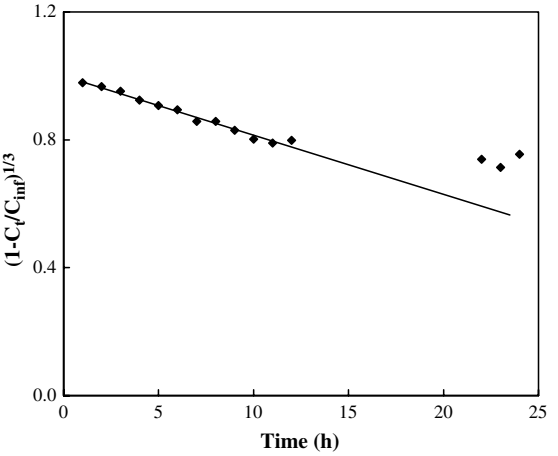

Fig. 3. Kinetics of chromium release from stellite #6.

does not dissolve along with the chromium – the particle size and shape is retained during the process of removal of chromium. It may be possible that, as the permanganic acid removes chromium from the stellite, the cobalt rich residue becomes highly porous and does not offer any resistance to the chromium dissolution reaction. SEM images were taken before and after exposure to $HMnO_4$ and are given in Fig. 4(a) and (b). From these images it is clear that after 24 h exposure to $HMnO_4$, the stellite particles seem to maintain their

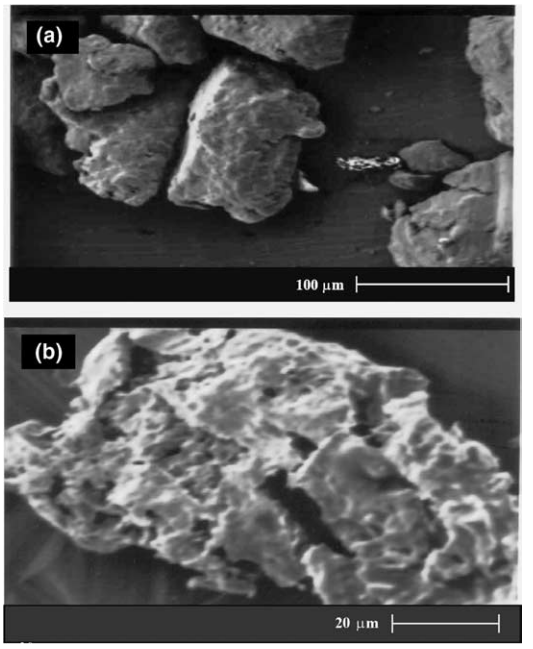

Fig. 4. SEM images of stellite #6 powder (a) unexposed and (b) exposed to oxidation pre-treatment with $HMnO_4$.

shape, but the surface morphology shows roughness and evidence of porosity. Thus, it was established that permanganic acid ($HMnO_4$) is efficient in dissolving the stellite #6. Complete dissolution of cobalt from stellite #6 can be ensured by repeated treatment with permanganic acid and citric acid/EAC.

In nuclear reactor coolant systems, the particles released from stellite #6 surfaces are in constant contact with water medium. Thus, it may be expected that oxidation of the surface of the stellite particles would have taken place and their dissolution behavior might be quite different from that of the stellite powder used here as it has not been exposed to water. Hence, the stellite #6 powder was exposed to neutral water at about 60 °C (similar to PHWR moderator condition) for about 10 days and dissolution experiment was carried out with this powder. This water-conditioned powder behaved in the same way as the powder that had not been conditioned. These observations indicate that in both cases the overall process takes place via in situ formation of Cr_2O_3 and its subsequent dissolution.

The dissolution behavior of stellite #6 was also investigated by measuring the corrosion rate of stellite #6. Stellite #6 rod was exposed to 2.5 mol/m^3 $HMnO_4$, which is the optimized concentration of the formulation, for 24 h followed by treatment with EAC for 3 h. The coupon was weighed before and after exposure to the full oxidation–complexation process, total duration of exposure being 28 h. The corrosion rate was found to be 0.033 μm/h.

Studies on the dissolution behavior of stellites #3 and #6 particles after they have been exposed to high-temperature water (250–315 °C) still need to be carried out. At high temperature, it has been reported that stellite gets covered with an oxide film of thickness 250 nm [12], which is significant considering the size of stellite particles (few microns). In addition, some of the stellite components are fabricated by a weld-deposition process. To what extent the weld deposition can affect the phase composition and its effect on dissolution needs to be studied further.

3.1.2. Dissolution of stellite #3

Dissolution studies carried out on stellite #6 were repeated with stellite #3. The latter alloy contains 12–13% tungsten, which makes it more resistant to chemical dissolution. The dissolution behavior of stellite #3 was studied with pre-treatment in varying concentrations of $HMnO_4$. It was observed that the dissolution of stellite #3 varied as the concentration of $HMnO_4$ was increased from 0.42 to 8.33 mol/m^3 (Fig. 5). In the concentration range of 0–1.25 mol/m^3, increasing the dissolution was observed with increasing concentration of permanganic acid. Maximum dissolution of stellite was observed at an $HMnO_4$ concentration range of 1.25–2.5 mol/m^3. Above 2.5 mol/m^3 the dissolution decreased with

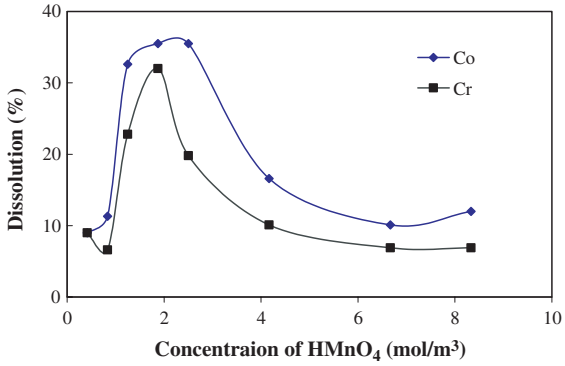

Fig. 5. Variation in stellite #3 dissolution with change in initial pre-treatment with different concentrations of $HMnO_4$, followed by treatment with ascorbic acid and EAC.

increasing concentration and reached a low value at 3.75 mol/m^3 concentration, thereafter it remained constant. This may be due to the formation of a passive film that hinders the dissolution process. Percentage dissolution at this region (3.75–8.33 mol/m^3) was almost constant indicating that the dissolution of stellite was mainly dependent on the film formed and that the nature of the passive film formed did not vary much with the further increase in concentration of permanganic acid. Conversely, the increase in the dissolution rate observed in the low-concentration region (0–2.5 mol/m^3) is attributed to the concentration dependent dissolution phenomenon. Thus, the optimum concentration of permanganic acid for the dissolution of stellite #3 is 1.25–2.5 mol/m^3.

The dissolution of stellite #3 with respect to time showed a similar trend to stellite #6, with cobalt coming into the solution only when the permanganic acid treated stellite was further treated with ascorbic acid/EAC. Ascorbic acid was used to neutralize the permanganic acid/MnO_2 remaining after the oxidation steps here as it was found to be quicker and consumes less chemicals than neutralization with the citric acid. Otherwise, the change to ascorbic acid as neutralizing agent does not have any other effect.

The amounts of both cobalt and chromium dissolved from stellite #3 during its exposure to permanganic acid were less than for the stellite #6. With 2.5 mol/m^3 $HMnO_4$, only 36% of the chromium could be dissolved in 24 h from stellite #3. The dissolution of chromium from stellite #3 also followed the cubic rate law, as evident from the plot of $(1 - C_t/C_\infty)^{1/3}$ vs time (Fig. 6), which is quite linear for the entire experimental duration of 24 h. In this case $k_{obs} = k/\rho r_o = 0.0026$ is almost one order of magnitude less than the measured value for stellite #6. Hence, the percentage of cobalt and chromium dissolved from stellite #3 is much less than for stellite #6. The slower kinetics for stellite #3 was evident from

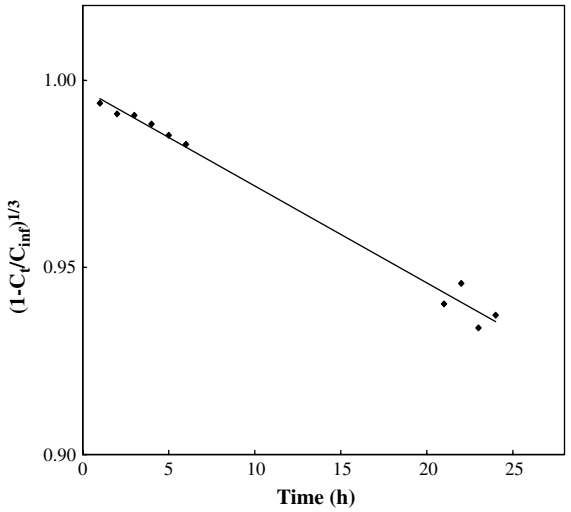

Fig. 6. Kinetics of chromium release from stellite #3.

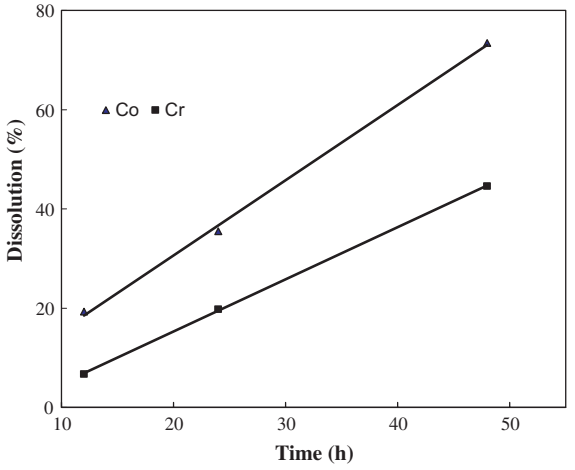

Fig. 7. Effect of pre-oxidation with 2.5 mol/m^3 $HMnO_4$ on release of cobalt and chromium from stellite #3.

a separate set of the experiments where the duration of oxidation step was increased from 12 to 24 h and then to 48 h. There was a linear increase in chromium release from stellite and the corresponding increase in cobalt release also was observed in the following ascorbic acid/EAC steps (Fig. 7). This observation again confirms that the release of cobalt from stellite #6 or #3 in the citric acid/ascorbic acid–EAC step is dependent upon the extent to which chromium is removed during the oxidative conditioning step.

3.1.3. Metal dissolution study with stellite #3 discs

The studies carried out on stellite powder were repeated with stellite #3 discs, using standard methods for studying the corrosion behavior of metals. Conventional weight-loss and electrochemical measurements helped to confirm the observations made with the powders. In addition, microscopic examination of the surface provided information on the nature of the residue left behind after the oxidation–complexation treatment. Overall stellite #3 dissolution was measured after the full oxidation–complexation cycle by weight loss method; all the results are listed in Table 3. The corrosion rate was higher if low concentrations of $HMnO_4$ were used in the pre-oxidation step. When the concentration of the formulation was increased to $\geqslant 2.5$ mol/m^3, as exemplified by the low-corrosion rate, the inferred passivation effect of the film could be observed.

The electrochemical polarization experiments were also carried out on stellite #3 discs in $HMnO_4$ media to study the film formed on stellite surface (Fig. 8). It was found that when the concentration of $HMnO_4$ was increased from 0.42 to 0.83 mol/m^3, the corrosion current increased. For $HMnO_4$ concentrations of $\geqslant 2.5$ mol/m^3, at the same potential, the current observed was less. There was also a shoulder on the anodic curve indicating passive film formation. At 0.2 mol/m^3, the $HMnO_4$ decomposed within 15 min rendering the data unreliable. The polarization studies complimented dissolution studies – both indicated that an $HMnO_4$ concentration of 2.5 mol/m^3 was approximately the boundary between active and passive region for stellite during oxidation. The corrosion/metal dissolution rates measured by the polarization method are given in Table 4.

Table 3
Corrosion rates of stellites #3 and #6 subjected to oxidative pre-treatment with different concentration of $HMnO_4$ at 90 °C

Material	Concentration of $HMnO_4$ (mol/m^3)	pH of the initial solution	Corrosion rate (μm/h)
Stellite #3	0.42–<0.42	3.56	0.0798
Stellite #3	0.42	3.56	0.0738
Stellite #3	0.42–0.75	3.56	0.0649
Stellite #3	2.5	2.7	0.015
Stellite #3	24	1.62	0.0146
Stellite #6	2.5	2.72	0.033

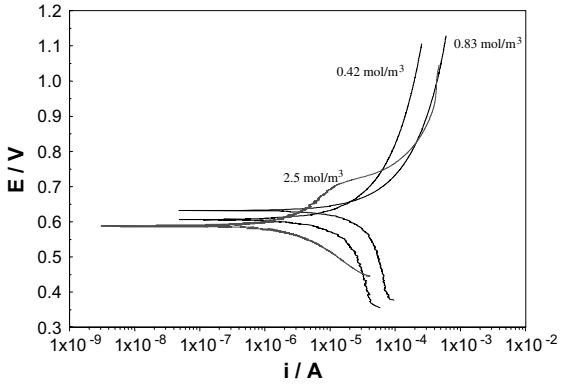

Fig. 8. Potentiodynamic polarization curves for stellite #3 in $HMnO_4$.

Table 4
Corrosion rates of stellite #3 as measured by electrochemical polarization exposed to different $HMnO_4$ concentrations

Material	$HMnO_4$ (mol/m^3)	Open circuit potential vs SCE (V)	Corrosion rate (μm/h)
Stellite #3	0.42	0.606	0.0374
Stellite #3	0.83	0.628	0.0621
Stellite #3	2.5	0.589	0.0073

3.2. Examination by SEM, EDX and XPS

3.2.1. Stellite #6

Unexposed stellite #6 rod was etched with H_2O_2 and HCl solution [5] after polishing to a diamond grade finish. Energy dispersive X-ray microanalysis (EDX) carried out on this etched specimen showed two different phases with cobalt rich dominant matrix phase (68% Co, 22% Cr) and chromium rich interdendritic phase (46% Cr, 41% Co). This type of microstructure for cast stellite #6 has also been explained elsewhere [3,5,6,12,13]. Elemental mapping of the unexposed specimen (by EDX) showed the association of oxygen with chromium in the interdendritic phase, which in turn indicates the presence of Cr_2O_3 in this particular region. Mapping of the specimen exposed only to $HMnO_4$ indicated transformation of Cr_2O_3 to chromate, which in turn is released to the solution as a soluble species. Subsequent to the removal of the thin Cr_2O_3 film, further oxidative dissolution of the chromium continues and the reminder becomes richer and richer in non-chromium elements. A SEM image recorded after this step (Fig. 9(a)) shows MnO_2 precipitate on the surface. Precipitation was found to occur mainly on the chromium depleted regions. The $HMnO_4$ medium, even though acidic, is not conducive for the dissolution of other metals because of its passive nature, hence the cobalt rich matrix seems to be practically unaffected by the $HMnO_4$ treatment.

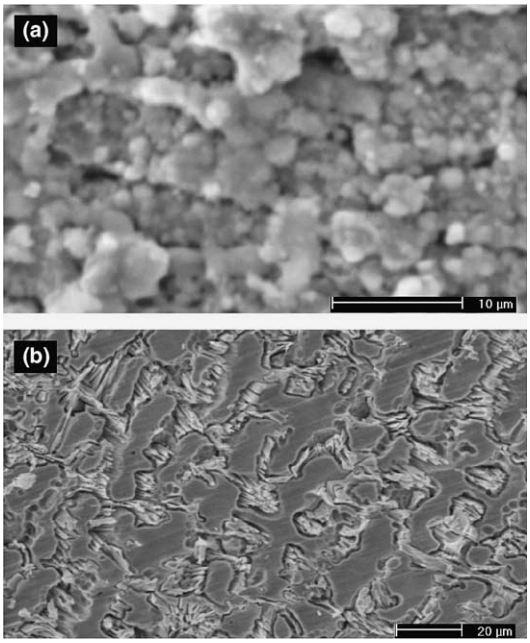

Fig. 9. SEM images of stellite #6 coupon exposed to 2.5 mol/m^3 $HMnO_4$ (a) showing MnO_2 precipitates and (b) after treatment with EAC.

Upon exposure to ascorbic acid, the MnO_2 precipitate dissolves and part of the cobalt and tungsten also dissolve in this acid medium. In the absence of passivating species like permanganate, the metals tend to dissolve by hydrogen liberation. The Co-rich matrix phase gets slightly depleted at this stage due to its preferential dissolution by ascorbic acid.

During the EAC step, the acid aided complexation–dissolution of the non-chromium metal ions such as cobalt, tungsten, etc., are favored. Hence, the chromium content in the Cr-rich grains, which were previously depleted of Cr by $HMnO_4$, increases and the overall composition tends to that of parent alloy (Table 5). However, the EAC formulation continues to dissolve cobalt until it is hindered by the chromium. Hence, exposure to EAC leaves a cobalt depleted (Cr enriched) surface. Essentially, after the full oxidation–complexation

Table 5
Distribution of elements in different phases in stellite #6 surface exposed to $HMnO_4$, ascorbic acid and EAC

Phase	Co (wt%)	Cr (wt%)	W (wt%)
Matrix	69.3	23.6	4.04
Inter-dendritic constituent	34.4	58.3	5.06

cycle, the alloy retains its original composition and structure except for the slight enrichment of chromium in Cr-rich grains. Fig. 9(b) shows the stellite #6 surface after EAC treatment. Exposure to the formulation has resulted in etching out the different phases that are present in the alloy.

3.3. Stellite #3

The EDX analyses carried out on an unexposed specimen indicated some chromium rich and some cobalt rich regions, but this was not as marked as in the case of stellite #6. An etched specimen showed overall chromium enrichment on the surface with no phase inhomogenity. The surface of a stellite #3 disc, after exposure to similar conditions to stellite #6, was black in appearance and a SEM image (Fig. 10(a)) shows a roughening pattern on the surface. A backscattered electron image showed that there was no phase inhomogenity, unlike in stellite # 6. Near the periphery of the disc, the SEM shows the structure corresponding to broken carbides (Fig. 10(b)). An EDX analysis showed that after the full oxidation followed by complexation process the surface was enriched in chromium (about 46% Cr). During oxidation, part of the chromium present on the surface (here, say about 36%) is oxidized and released into the solution, leaving behind a surface that is rich in cobalt and containing some undissolved chromium. In the EAC step, cobalt is released to the solution leaving the Cr unaffected. As no chromium comes out in this step, the surface becomes enriched with chromium. This was proved by XPS analysis of the exposed surface. X-ray photoelectron surface analysis was carried out on stellite #3 disc that had been treated with permanganic acid followed by ascorbic acid and EAC. The Co 2p and Cr 2p spectra before and after exposure are compared in Fig. 11. It can be seen that cobalt is altogether missing from the surface after the exposure, whereas chromium is still left indicating a Cr-rich surface. The spectra of both unexposed as well as exposed specimens shows $2p_{3/2}$ peaks corresponding to Cr_2O_3 along with $2p_{3/2}$ peaks of metallic chromium with binding energies of 576.68 and 574.02 eV respectively after correction for surface charging.

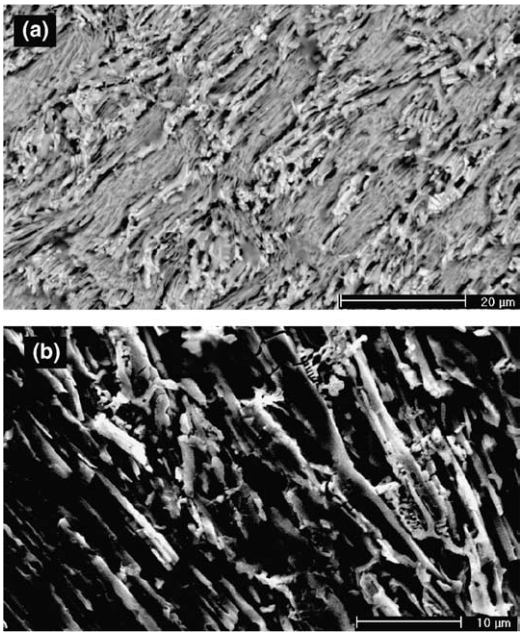

Fig. 10. SEM images of stellite #3 coupon exposed to 2.5 mol/m^3 $HMnO_4$ and EAC (a) center region and (b) periphery.

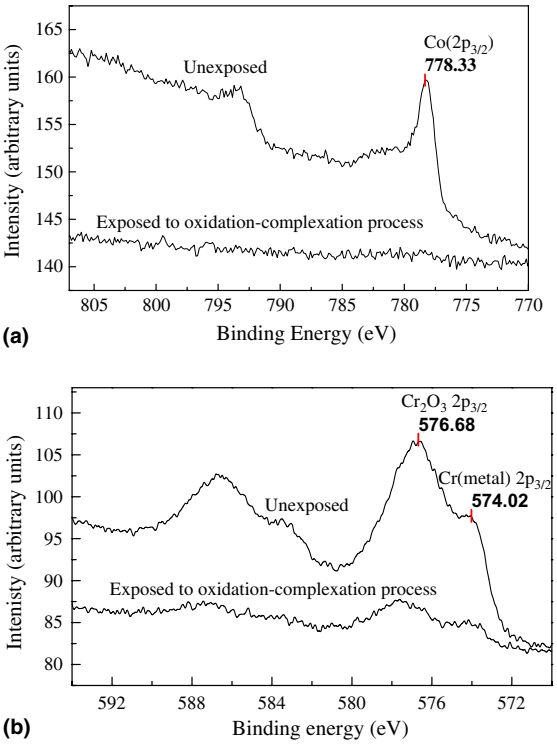

Fig. 11. XPS spectra of stellite #3 surface showing (a) Co $2p_{3/2}$ peak and (b) Cr $2p_{3/2}$ peak corresponding to exposed and unexposed specimen.

3.4. XRD studies

Different phases present in the stellites were identified by X-ray powder diffraction technique using the Cu K_α line; mainly chromium rich carbides of type $M_{23}C_6$ and M_7C_3 were identified. As can be seen from Fig. 12, there is no significant variation in the number of peaks in the XRD patterns for stellite #6 before and after exposure. Though Cr_2O_3 may also be present, its concentration will not be significant in comparison to

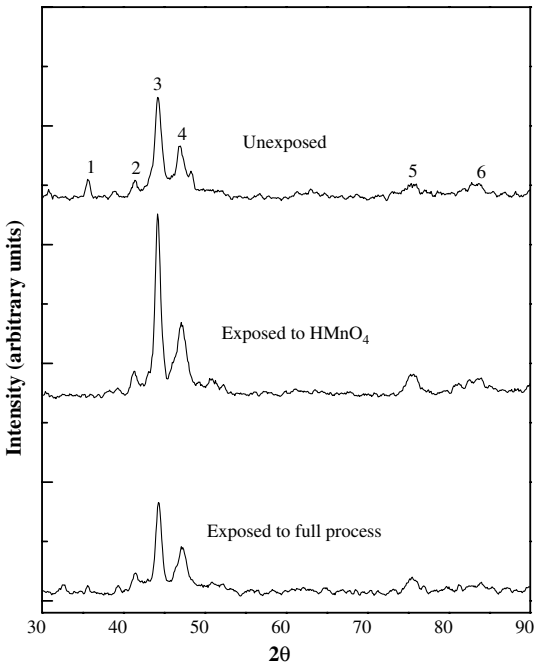

Fig. 12. XRD pattern of stellite #6 before and after exposure to 2.5 mol/m^3 $HMnO_4$ and after exposure to EAC.

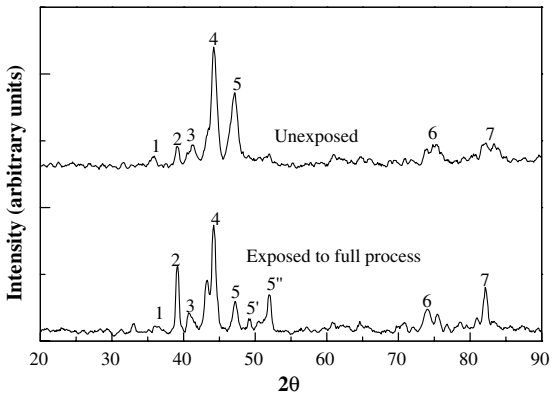

Fig. 13. XRD pattern of stellite #3 before and after exposure to 2.5 mol/m^3 $HMnO_4$ followed by treatment with EAC.

the bulk carbides. The similarity in XRD patterns of stellite #6 before and after exposure to $HMnO_4$ shows that during oxidation Co remains as it is in the original alloy without getting oxidized. However, slight variations in the intensity ratios of the peaks were observed, and are listed in Table 6 along with the list of phases identified.

Table 6
Different phases and their relative intensity ratios for stellite #6 from its XRD pattern

Stellite #6			Relative intensity of peaks (I/I_{max})		
Peak no.	2θ	Phases	Unexposed	Exposed to $HMnO_4$	Exposed to complete process
1	35.6	WC (100)	25	–	15
2	41.4	$Cr_{23}C_6$ (422)	25	17	28
3	44.2	$Cr_{23}C_6$ (511), Cr_7C_3 (151), Co_3C (101)	100	100	100
4	47.0	$Cr_{23}C_6$ (440)	56	43	55
5	75.7	$Cr_{23}C_6$ (660)	21	16	24
6	82.8	$Cr_{23}C_6$ (911)	22	12	19

Table 7
Different phases and their relative intensity ratios for stellite #3 from its XRD pattern

Stellite #3			Relative intensity of peaks (I/I_{max})	
Peak no.	2θ	Phases	Unexposed	Exposed
1	35.7	WC (100)	14	–
2	39.1	Cr_3C_2 (121)	22	64
3	41.2	$Cr_{23}C_6$ (422), Co_3C (002)	23	24
4	44.2	$Cr_{23}C_6$ (511), Cr_7C_3 (151), Co_3C (101)	100	100
5	47.1	$Cr_{23}C_6$ (440)	64	34
5′	49.1	Cr_7C_3 (331)	–	19
5″	52.0	$Cr_{23}C_6$ (442)	–	40
6	75.4	$Cr_{23}C_6$ (660)	23	23
7	82.2	$Cr_{23}C_6$ (911)	24	46

For stellite #3, a few more lines appeared in the XRD pattern for the sample that was exposed to the full oxidation–complexation cycle as compared to the starting material (Fig. 13). Table 7 gives the 2θ values of the peaks observed and the phases associated with them as well as the relative intensities of secondary peaks with respect to the major peak. Changes in the relative intensities of the peaks before and after exposure suggests preferential dissolution of certain planes.

These data indicate that there are some phases in stellite #3, which cannot be dissolved, in permanganic acid–ascorbic acid–EAC reagents. However, analysis of the dissolution data indicated that the residue contains very much less cobalt. As complete dissolution of cobalt rather than complete dissolution of stellite is the requirement as far as chemical decontamination of hot spots is concerned, this residue is not going to have any significant effect on the removal of cobalt activity.

4. Summary and conclusions

(1) Oxidizing pre-treatment with acidic permanganate helps in the dissolution of stellite #6 as well as stellite #3 by chemical decontamination reagents. Permanganic acid is more effective as an oxidizing pre-treatment agent as than the nitric acid–permanganate.
(2) During the oxidation step only chromium is released from stellite. Cobalt and other elements are released to the solution during the subsequent treatment with neutralizing agent and complexing acid(s).
(3) Kinetically dissolution of stellite #6 is faster than to stellite #3, but the dissolution of the latter can be ensured by repeated application of oxidation–complexation cycles.
(4) No observable oxidation of cobalt occurs in stellites during the oxidation step. It dissolves almost completely in stellite #6 and partially in stellite #3 in media containing complexing acid, probably due to destabilization of the matrix that occurs due to oxidation and removal of chromium from the alloy.
(5) Some insoluble carbide residues are left behind during the dissolution of stellite #3 in permanganic acid–ascorbic acid–EAC; however, this insoluble residue contains hardly any cobalt.

References

[1] http://www.weartech.net/WEARTECH.pdf.
[2] V. Kuzuku, M. Ceylan, H. Celik, I. Aksoy, J. Mater. Process. Technol. 79 (1998) 47.
[3] J.L. De Mol VanOtterloo, J.Th.M. De Hosson, Acta Mater. 45 (3) (1997) 1225.
[4] E. Lemaire, M. Le Calvar, Wear 249 (2001) 338.
[5] L. Wang, D.Y. Li, Wear 255 (2003) 535.
[6] Rocher, P. Ridoux, S. Anthoni, C. Brun, Programme to eradicate hot Spots (Co-60) carried out in french PWR units, 1st EC/ISOE workshop on occupational exposure management at NPPS, Malmö, Sweden, 16–18 September 1998.
[7] M.G. Segal, T. Swan, Water Chem. Nuclear React. Syst. 1 (3) (1983) 141.
[8] M.E. Pick, Water Chem. Nuclear React. Syst. 1 (3) (1983) 61.
[9] J.Schunk, J.Makai J. Kreisz, A. Krojer, P. Komaromi, I. Schremmer, T. Szanya, L. Hanak, G. Simon, Qualification of a low concentration method for decontamination of primary systems, IAEA-TECDOC-1022 New methods and techniques for decontamination in maintenance or decommissioning operations, 95-107, June 1998.
[10] V.M. Efremenkov, N.I. Voronik, N.V. Shatilo, Decontamination as a part of decommissioning and maintenance work at nuclear installations, IAEA-TECDOC-1022 New methods and techniques for decontamination in maintenance or decommissioning operations, 95-107, June 1998.
[11] A.B. O'Brien, M.G. Segal, W.J. Williams, Chem. Soc. Faraday Trans. cas1 83 (1987) 371.
[12] N.K. Taylor, I. Armson, Water Chem. Nuclear React. Syst. 1 (3) (1983) 141.
[13] W.H. Hocking, F.W. Stanchell, E. McAlpine, D.H. Lister, Corrosion Sci. 25 (7) (1985) 531.